Steam treatment on Ni/γ-Al$_2$O$_3$ for enhanced carbon resistance in combined steam and carbon dioxide reforming of methane

In Hyuk Son [a,*], Seung Jae Lee [a], Aloysius Soon [b], Hyun-Seog Roh [c], Hyunjoo Lee [d,**]

[a] Environment Group, Energy Lab, Samsung Advanced Institute of Technology (SAIT), Samsung Electronics Co. Ltd., Gyounggi-Do 446-712, Republic of Korea
[b] Department of Materials Science and Engineering, Yonsei University, Seoul 120-749, Republic of Korea
[c] Department of Environmental Engineering, Yonsei University, Wonju, Gangwon-do 220-710, Republic of Korea
[d] Department of Chemical and Biomolecular Engineering, Yonsei University, Seoul 120-749, Republic of Korea

ARTICLE INFO

ABSTRACT

Coke deposition on reforming reaction catalysts, typically Ni particles deposited on alumina supports, has been a major obstacle barring their practical industrial application. In this work, a Ni/γ-Al$_2$O$_3$ catalyst was stabilized by a pretreatment with steam at high temperature of 850 °C. The steam-treated Ni/γ-Al$_2$O$_3$ catalyst showed thermodynamically possible highest conversion (98.3% for methane and 82.4% for carbon dioxide) and H$_2$/CO ratio of 2.01 for combined steam and carbon dioxide reforming of methane, and operated stably for 200 h. The amount of deposited carbon coke was 3.6% for steam-treated catalysts whereas conventional catalysts had 15.4% of coke after 200 h of the reaction. The steam pretreatment removed unstable aluminum that can otherwise leach out, which causes severe carbon deposition at the early stage of the reaction. This novel steam pretreatment enhanced the carbon resistance of the catalysts significantly, resulting in improved activity and long-term stability.

© 2013 Elsevier B.V. All rights reserved.

1. Introduction

The methane reforming reaction has attracted much attention as a way to produce hydrogen practically and, more importantly, to produce artificial petroleum in connection with the Fischer–Tropsch reaction. Compared to depleted crude oil, the reservoir for methane is still significant from natural gas, shale gas, methane hydrates, livestock excretion, fermented waste, and other sources [1]. When methane reacts with steam or carbon dioxide, a mixture of hydrogen and carbon monoxide, also called syn-gas, can be produced. Methane reforming with carbon dioxide has been in the limelight recently due to its potential to reduce greenhouse gases [2–4]. Syn-gas is used as a reactant to prepare long-chain hydrocarbons via the Fischer–Tropsch reaction. The ratio of hydrogen to carbon monoxide in syn-gas is three for steam reforming (CH$_4$ + H$_2$O → 3H$_2$ + CO), and one for dry reforming (CH$_4$ + CO$_2$ → 2H$_2$ + 2CO). However, a ratio of two is preferred when syn-gas is directly used in the Fischer–Tropsch reaction (($2n + 1$)H$_2$ + nCO → C$_n$H$_{(2n+2)}$ + nH$_2$O; n should be large for desired oily products, then ($2n + 1$)/n converges to 2). Combined steam and carbon dioxide reforming of methane can easily control the ratio of hydrogen to carbon monoxide by altering the ratio of the reactants (methane, steam, and carbon dioxide) in the inlet flow [5]. When the ratio of methane to steam to carbon dioxide is 1:0.8:0.4 in the inlet, the theoretical ratio of hydrogen to carbon monoxide in the outlet can be two [6].

The typical catalyst for methane reforming is composed of Ni particles deposited on an alumina support. Many commercial Ni/Al$_2$O$_3$-based catalysts are available for fuel re-forming, such as Ni-0309S (Engelhard Company), ICI-46-1 (Imperial Chemical Industries), and FCR-4 (Sud-Chemie). These catalysts are relatively cheap because precious metals are not used and can operate stably with high activity under excess steam [7]. However, when steam is not in excess and carbon dioxide is used, severe carbon deposition is observed on the Ni/Al$_2$O$_3$ catalyst [8]. Extensive research has been performed to minimize carbon coke formation by synthesizing a Ni alloy with other transition metals such as Cu, Co, Sn, Mn [9–12], or by using a strong metal-support interaction with supports such as CaO, TiO$_2$, CeO$_2$, ZrO$_2$, and MgO [13–18]. The direct control over Ni particle size was also tried to minimize coke formation [19].

In this work, we investigated the effect of steam pretreatment for the combined steam and carbon dioxide reforming of methane. The conversion of methane and carbon dioxide, the ratio of hydrogen to carbon monoxide, and the carbon deposition on the catalyst

were examined after pretreating the Ni/γ-Al$_2$O$_3$ catalysts with steam at high temperature. The enhancement in activity and long-term stability has been pursued by this simple treatment.

2. Experimental procedures

2.1. Preparation of catalysts

A 7 wt% Ni/Al$_2$O$_3$ catalyst was prepared using the incipient wetness method. γ-alumina (S_{BET} = 150 m^2/g, ~3 mm φ; Aldrich) was impregnated using an aqueous solution of Ni(NO$_3$)$_2$·6H$_2$O (Aldrich). The catalyst was dried in an oven at 120 °C for 24 h and calcined in air (300 mL/min) at 500 °C for 5 h. The calcined catalyst was reduced in pure H$_2$ with increasing temperature (10 °C/min) and maintained at 850 °C for 2 h. This is considered the *conventional pretreatment*. In the *steam pretreatment*, the reactor was cooled to around 30 °C and about 1 g of the catalyst was again reduced in a gas flow (1.2 L/min) with a 1:3 mixture of H$_2$/H$_2$O with increasing temperature (7 °C/min), and then maintained at 850 °C for 2 h.

2.2. Catalytic activity test

The prepared catalyst (0.45 g, 10–20 mesh) diluted with α-alumina (4.45 g, S_{BET} = 10 m^2/g, ~3 mm φ; Aldrich) was charged in a fixed-bed quartz reactor (I.D. = 7 mm). Before the reaction, the catalyst was reduced at 850 °C for 1 h under a mixture of 20% H$_2$ in N$_2$ at a flow rate of 200 mL/min. A gas hourly space velocity (GHSV) of 50,666 ml/g/h was used with the desired reaction gas mixture composition (CH$_4$:CO$_2$:H$_2$O:N$_2$ = 1:0.4:0.8:1.6) to obtain a product H$_2$:CO ratio of two. The liquid water (0.065 mL/min) was provided to evaporator by using HPLC pump (Chrom Tech, Inc. Series 1500, USA). Then the generated steam (80 mL/min) was mixed with the other gases (CH$_4$ 100 mL/min, CO$_2$ 40 mL/min, N$_2$ 160 mL/min at standard condition of 1 atm and 273 K) and fed into the reactor. The actual flow rate of the gaseous reactants was adjusted depending on the room temperature. The reforming reaction was carried out by increasing the temperature from 700 °C to 850 °C at a rate of 2.5 °C/min under atmospheric pressure. N$_2$ was used to calculate CH$_4$ conversion as an internal standard. The effluent was passed through a trap to condense residual steam and analyzed using an on-line IR-gas analyzer (NGA2000, MLT4, Rosemount Analyzer System from Emerson Process Management; CO at ppm level, CO$_2$, H$_2$, and CH$_4$ at 0.01 percent level). Turnover frequency (TOF) of CH$_4$ and CO$_2$ was estimated by dividing the mole number of CH$_4$ or CO$_2$ reacted per unit time by the mole number of H$_2$ uptake on the catalyst for the same mass of the catalyst. The conversion of CH$_4$ and CO$_2$, the yield of H$_2$ and CO, and H$_2$/CO ratio were calculated using the following formulas.

$$CH_4 \ \ conversion = \frac{[CH_4]_{in} - [CH_4]_{out}}{[CH_4]_{in}} \times 100$$

$$CO_2 \ \ conversion = \frac{[CO_2]_{in} - [CO_2]_{out}}{[CO_2]_{in}} \times 100$$

$$H_2 \ \ yield = \frac{[H_2]_{out}}{[CH_4]_{in} \times 2 + [H_2O]_{in}} \times 100$$

$$CO \ \ yield = \frac{[CO]_{out}}{[CH_4]_{in} + [CO_2]_{in}} \times 100$$

$$H_2/CO \ \ ratio = \frac{[H_2]_{out}}{[CO]_{out}}$$

Long-term stability was tested by running the reaction at 850 °C for 200 h at otherwise the same condition.

2.3. Characterization

The BET surface area and pore volume of the catalysts were measured by N$_2$ adsorption at −196 °C using a BET instrument (BELsorp, BEL, Japan). Approximately 0.1 g of catalyst was used for each analysis. The degassing temperature was 200 °C to remove the moisture and other adsorbed gases from the catalyst surface. X-ray diffraction (XRD) was performed using a Philips X'pert Pro X-ray diffractometer with nickel-filtered CuKα radiation (40 kV tube voltage and 40 mA tube current) at a 4°/min scan rate and 0.02° data interval. The crystalline size of the Ni particle was calculated from the XRD pattern of the catalysts using the Debye–Scherrer's equation. H$_2$ chemisorption was conducted using Micrometrics ASAP 2010. The calcined catalyst sample (about 0.1 g) was reduced at 800 °C for 1 hr in an H$_2$ flow and analyzed at 50 °C. Each point was measured after 5 min stabilization. The Ni surface area was calculated from the chemisorbed amount by assuming an adsorption stoichiometry of one hydrogen atom per nickel surface atom (H/Ni$_s$ = 1). NH$_3$ temperature-programmed desorption (TPD) was performed on a Chemisorption Analyzer (BEL-CAT). The catalyst (50 mg) was activated at 400 °C for 1 h under He flow (30 ml/min) and then cooled to 50 °C. The NH$_3$ flow was maintained for 1 h, and the sample was then flushed with He to remove any physisorbed NH$_3$. The desorption profile was recorded by increasing the sample temperature at a ramp rate of 10 °C/min. The NH$_3$ concentration in the effluent stream was monitored with a thermal conductivity detector, and the areas under the peaks were integrated to determine the amount of desorbed NH$_3$ during TPD. Temperature-programmed reduction (TPR) was performed on a Chemisorption Analyzer (BEL-CAT). The catalyst (50 mg) was pre-treated at 250 °C for 1 h under Ar flow (50 ml/min) and then cooled to room temperature. The catalyst was re-heated with a ramping rate of 10 °C/min and a flow rate of 50 ml/min up to 1000 °C under 5% H$_2$ in Ar gas. The quantitative analysis of the coke on the used catalyst was performed with a thermogravimetry analyzer (METTLER TOLEDO TGA/DSC1). The sample of 50 mg was heated from 30 to 850 °C with a heating rate of 5 °C/min in air. The electronic states of fresh catalysts were measured using an X-ray photoelectron spectroscope (XPS, ESCA 2000) equipped with a monochrometer (quartz), a twin X-ray source (Mg/Al target), and a hemispherical analyzer. The binding energy was calculated with respect to the maximum intensity of the C 1s signal at 284.6 eV. The catalysts were also examined using transmission electron microscopy (TEM; TITAN-80-300, FEI) operated at 300 kV and ultra-high-resolution field emission scanning electron microscopy (UHR-FE-SEM; Hitachi S-5500, resolution 0.4 nm) operating at 30 kV. Elemental composition was assessed using energy dispersive X-ray spectroscopy (EDS) in conjunction with UHR-FE-SEM. The specimens for EM characterization were prepared by spreading a droplet of ethanol suspension containing the sample onto a copper grid coated with a thin layer of amorphous carbon film and allowing it to dry in air.

3. Results and discussion

Table 1 shows BET surface area, pore volume, and size of Ni nanoparticles in fresh NiAl and WNiAl catalysts. After steam pretreatment, surface area decreased from 130.3 m^2/g to 93.7 m^2/g, but pore volume increased from 0.34 cm^3/g to 0.45 cm^3/g, respectively. The average size of the Ni nanoparticles was estimated using both H$_2$ chemisorption and XRD; the two values were reasonably close. The size of Ni nanoparticles increased significantly after steam pretreatment. Fig. 1(a) and (c) shows representative TEM images of fresh NiAl and WNiAl catalysts. While it is difficult to distinguish Ni nanoparticles in the NiAl catalyst, probably due to their

Table 1
Physical properties of the catalysts. The used catalysts indicate after 200 h of combined reforming reaction of methane.

Catalyst	BET surface area	Pore volume	^{27}Al NMR peak area ratio	Ni crystallite diameter (nm)	
	(m^2/g)	(cm^3/g)	(Al_{Td}/Al_{Oh})	By H_2 chemisorption	By XRD[a]
Fresh NiAl	130.3	0.34	0.37	4.2	6.5
Used NiAl	46.0	0.15	0.27	23.5	21.8
Fresh WNiAl	93.7	0.45	0.38	17.3	16.5
Used WNiAl	68.6	0.39	0.33	19.6	19.5

[a] Data obtained from Ni(2 2 0) diffraction peak broadening using the Scherrer equation.

small size, the WNiAl catalyst displayed distinct Ni nanoparticles with a size of greater than 10 nm.

Combined steam and carbon dioxide reforming of methane was performed with these catalysts at atmospheric pressure using a gas hourly space velocity (GHSV) of 50,666 ml/g/hr. The composition of inlet gas was $CH_4:CO_2:H_2O:N_2 = 1:0.4:0.8:1.6$. Fig. 2 shows the CH_4 and CO_2 conversion and H_2/CO ratio at various temperatures. Dotted lines indicate thermodynamic values for the conversion and the ratio at the given temperatures, as calculated by Outokumpu HSC chemistry software. Generally, WNiAl catalysts exhibited improved conversion over NiAl catalysts. WNiAl catalysts especially exhibited much higher conversion of carbon dioxide and lower H_2/CO ratio at low temperatures of 700–750 °C. Carbon dioxide seemed to convert to carbon monoxide, possibly via a reverse Boudouard reaction

with carbon coke ($C + CO_2 \rightarrow 2CO$) [20]. CH_4 and CO conversion and the H_2/CO ratio for WNiAl catalysts approached thermodynamic values at 850 °C.

Long-term stability was tested at 850 °C for 200 h, after which severe carbon deposition was observed for the NiAl catalysts as shown in Fig. 1(b). Wire-type deposited carbon is clearly visible. Ni nanoparticle size increased from 4.2 nm to 23.5 nm, as measured by H_2 chemisorption. Large Ni nanoparticles were also clearly observed in the TEM image in Fig. 1(b). On the other hand, wire-type carbon coke was not observed in the WNiAl catalyst after the reforming reaction for 200 h, as shown in Fig. 1(d). The size of Ni nanoparticles increased only slightly, from 17.3 nm to 19.6 nm. Fig. 3 shows CH_4 and CO_2 conversion and the H_2/CO ratio over 200 h of combined steam and carbon dioxide reforming of methane.
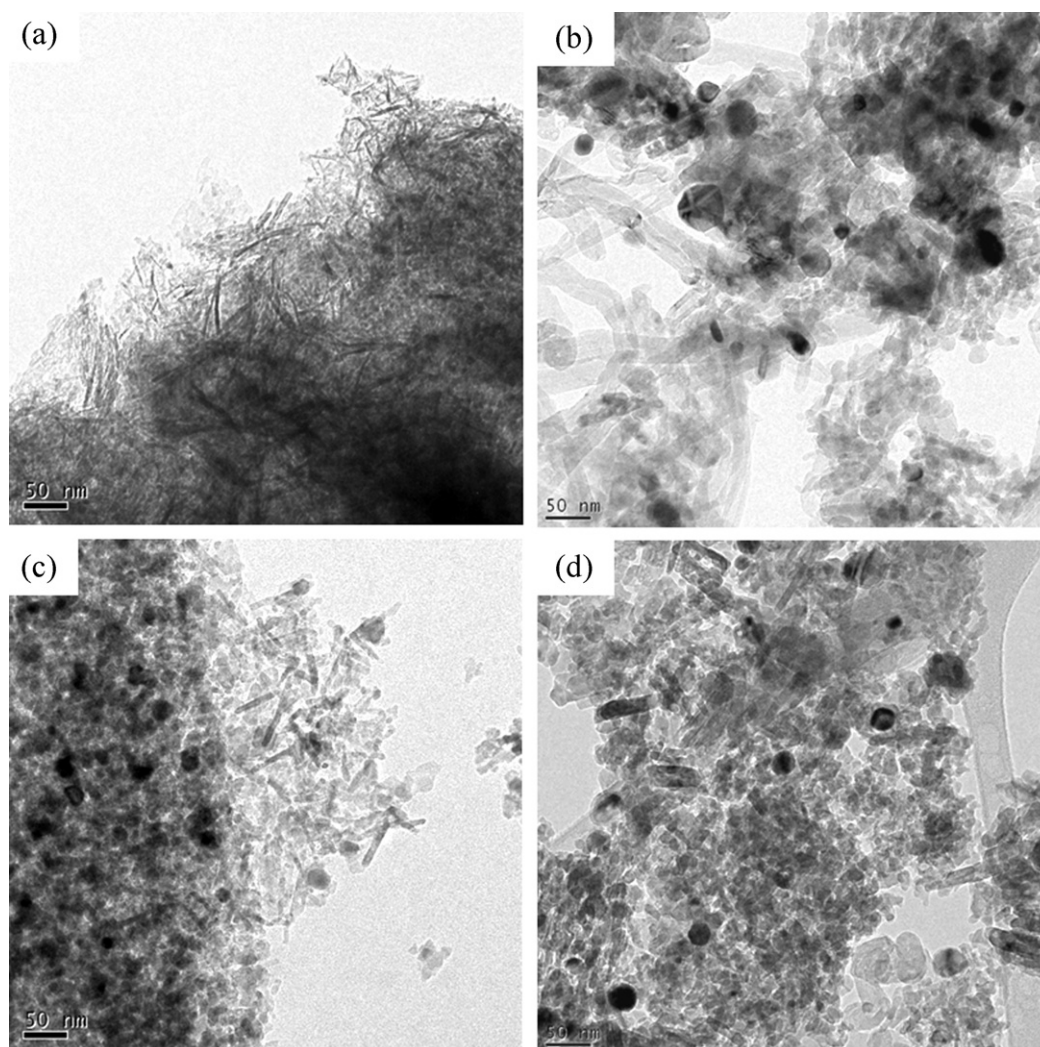

Fig. 1. TEM images of catalysts: (a) fresh Ni/γ-Al$_2$O$_3$ (NiAl), (b) used NiAl, (c) fresh steam-treated Ni/γ-Al$_2$O$_3$ (WNiAl), and (d) used WNiAl. The used catalysts indicate after 200 h of combined reforming reaction of methane.

Table 2
Reaction data of the catalysts. The used catalysts indicate after 200 h of combined reforming reaction of methane.

	Ni disp[a] (%)	CH$_4$ conv	CO$_2$ conv	TOF$_{CH4}$ (s^{-1})	TOF$_{CO2}$ (s^{-1})	H$_2$ Yield	CO Yield	H$_2$/CO ratio
Fresh NiAl	22.9	94.1	76.1	3.06	0.99	91.0	86.8	2.08
Used NiAl	4.1	90.8	73.3	16.36	5.28	88.9	81.7	2.16
Fresh WNiAl	5.6	98.3	82.4	13.01	4.36	93.8	93.5	2.01
Used WNiAl	5.0	97.1	81.2	14.60	4.88	92.4	91.5	2.03

[a] Dispersion measured by H$_2$ adsorption.
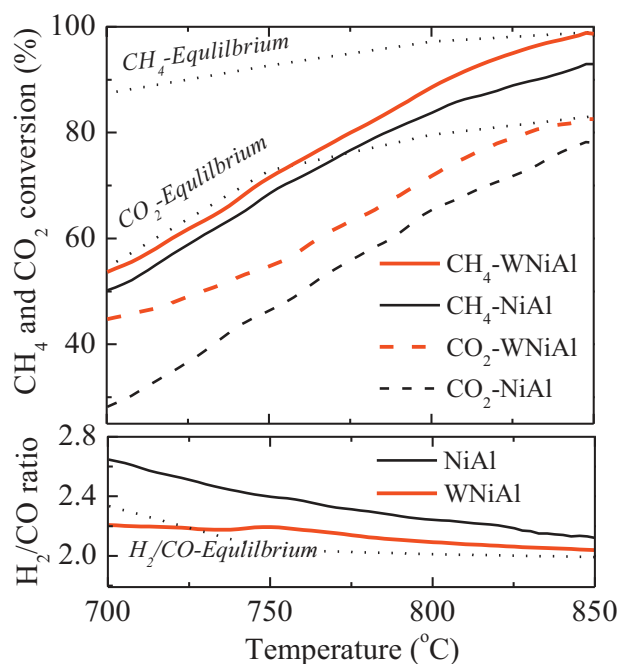
Fig. 2. CH$_4$ and CO$_2$ conversion and H$_2$/CO ratio of NiAl and WNiAl catalysts with various temperatures (reaction conditions: P = 1 atm, GHSV = 50,666 ml/g/h, CH$_4$:CO$_2$:H$_2$O:N$_2$ = 1:0.4:0.8:1.6).
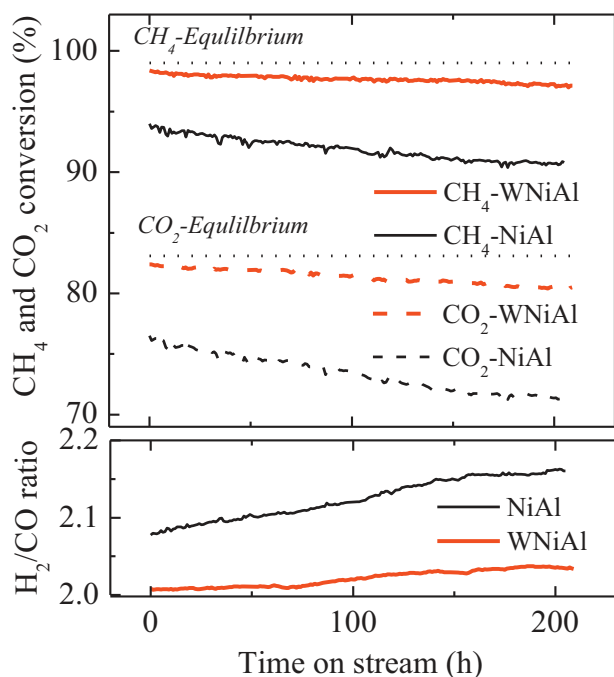

Fig. 3. CH$_4$ and CO$_2$ conversion and H$_2$/CO ratio of NiAl and WNiAl catalysts over 200 h of reaction (reaction conditions: 850 °C, P = 1 atm, GHSV = 50,666 ml/g/h, CH$_4$:CO$_2$:H$_2$O:N$_2$ = 1:0.4:0.8:1.6).
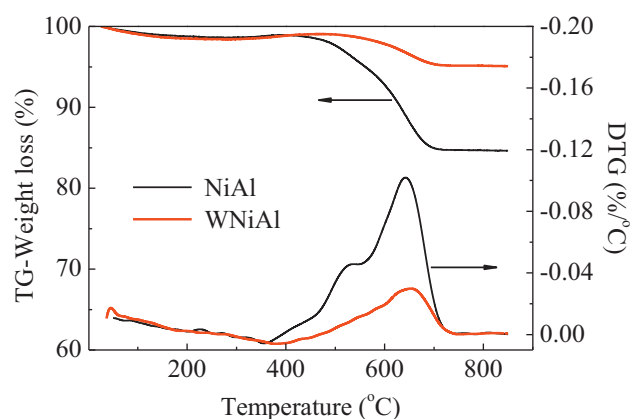

Fig. 4. Thermogravimetric and differential thermogravimetric profile of NiAl and WNiAl catalysts after 200 h of reaction (reaction conditions: 850 °C, P = 1 atm, GHSV = 50,666 ml/g/h, CH$_4$:CO$_2$:H$_2$O:N$_2$ = 1:0.4:0.8:1.6).

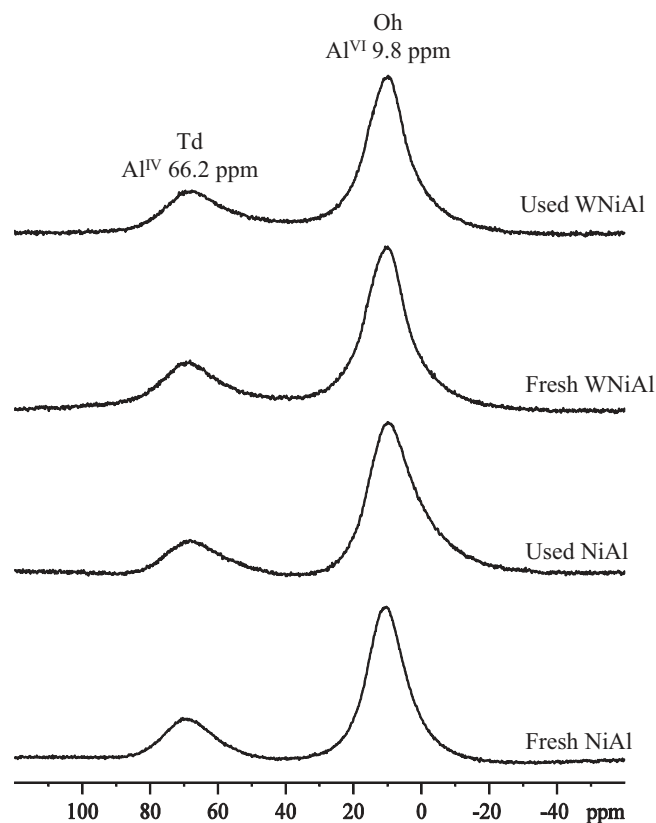**Fig. 5.** ^{27}Al MAS-NMR spectra of NiAl and WNiAl catalysts before and after the reaction (reaction conditions: 850 °C, P = 1 atm, GHSV = 50,666 ml/g/h, CH$_4$:CO$_2$:H$_2$O:N$_2$ = 1:0.4:0.8:1.6). The used catalysts indicate after 200 h of combined reforming reaction of methane.
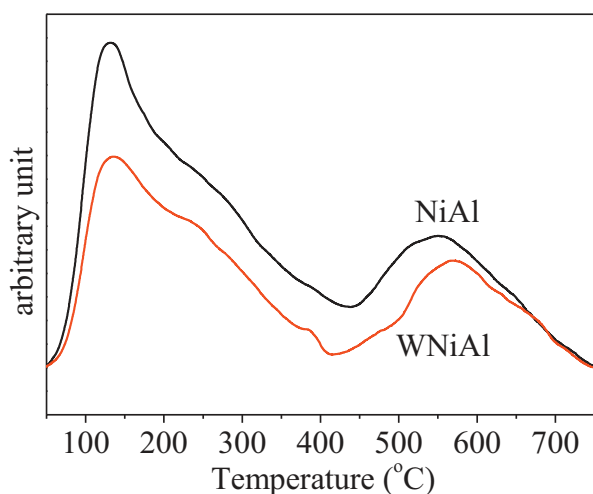
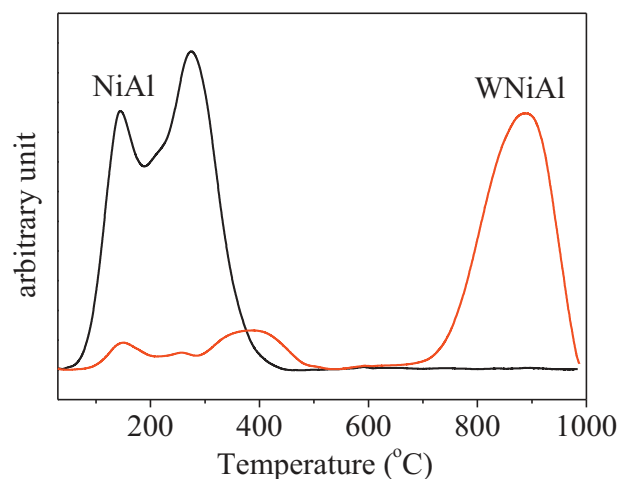**Fig. 6.** NH$_3$-TPD results for fresh NiAl and fresh WNiAl catalysts.

Fig. 7. TPR results for fresh NiAl and fresh WNiAl catalysts.

For the tested gas compositions, the equilibrium conversion of methane and carbon dioxide was calculated as 99.0% and 83.1%, respectively. Initially, the WNiAl catalyst showed nearly equilibrium conversion; 98.3% for methane and 82.4% for carbon dioxide. The ratio of hydrogen to carbon monoxide was 2.01, very close to the desired value of two. After 200 h of the reforming reaction, conversion slightly decreased to 97.1% for methane and 81.2% for carbon dioxide. The ratio of hydrogen to carbon monoxide increased slightly to 2.03. However, for the NiAl catalyst, initial conversion was significantly lower: 94.1% for methane and 76.1% for carbon dioxide. The ratio of hydrogen to carbon monoxide was higher, at 2.08. After 200 h, conversion decreased to 90.8% for methane and 73.3% for carbon dioxide, and the ratio of hydrogen to carbon monoxide increased to 2.16. The changes in Ni dispersion, turnover frequency (TOF), and the yields of H$_2$ and CO are summarized in Table 2. When TOF of the fresh catalysts were compared, WNiAl had much higher number than NiAl catalysts (13.01 vs. 3.06). After 200 h of the combined reforming reaction of methane, the Ni dispersion decreased greatly for NiAl catalysts from 22.9% to 4.1%, whereas the reduction was minimized for WNiAl catalysts from 5.6% to 5.0%.

The carbon deposited on the catalyst was examined. Fig. 4 shows thermogravimetric weight loss and a differential thermogravimetric profile of the catalysts after 200 h of the reforming reaction. Weight loss was much greater for the NiAl catalyst (15.4%) as compared to the WNiAl catalyst (3.6%). Much more carbon coke was formed on the conventional NiAl catalyst during the reforming reaction. The change in BET surface area and pore volume also confirmed more severe carbon deposition on the conventional NiAl catalyst. The surface area of the NiAl catalyst was reduced from 130.3 m^2/g to 46.0 m^2/g, but it was reduced from 93.7 m^2/g to 68.6 m^2/g in the WNiAl catalyst. Pore volume decreased from 0.34 cm^3/g to 0.15 cm^3/g for the NiAl catalyst, but it showed only a slight reduction, from 0.45 cm^3/g to 0.39 cm^3/g, for the WNiAl catalyst. The deposited coke blocked the porous structure in the conventional NiAl catalyst much more. The initial carbon deposition was measured for the catalysts after only 10 h of the reaction. The weight loss was 7.7% for the conventional NiAl catalyst but only 0.7% for the WNiAl catalyst. The carbon deposition rate was initially 7.7 mg C/gcat/h for NiAl and 0.7 mg C/gcat/h for WNiAl, whereas the average carbon deposition rate was 0.77 mg C/gcat/h for NiAl and 0.18 mg C/gcat/h for WNiAl over 200 h. The majority of the carbon coke was formed at an early stage of the reforming reaction, as
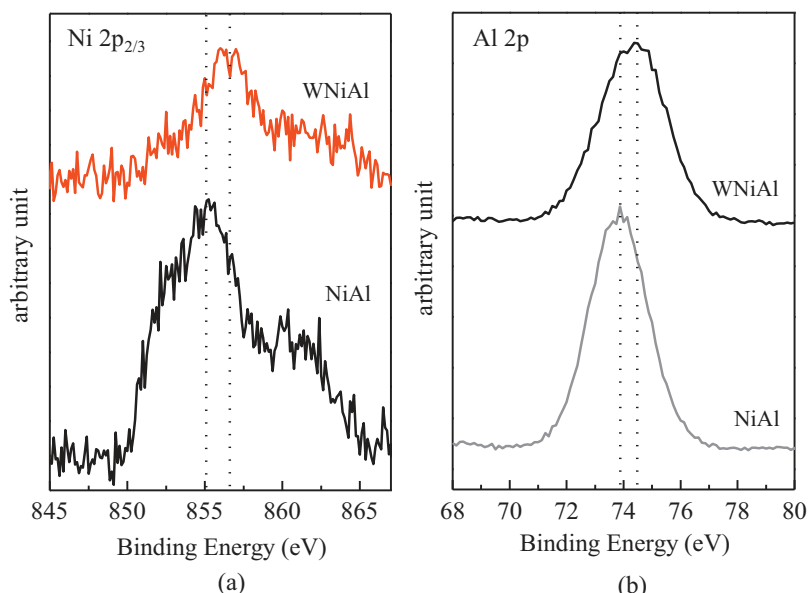

Fig. 8. XPS spectra of (a) Ni 2p$_{2/3}$ and (b) Al 2p for fresh NiAl and fresh WNiAl catalysts.
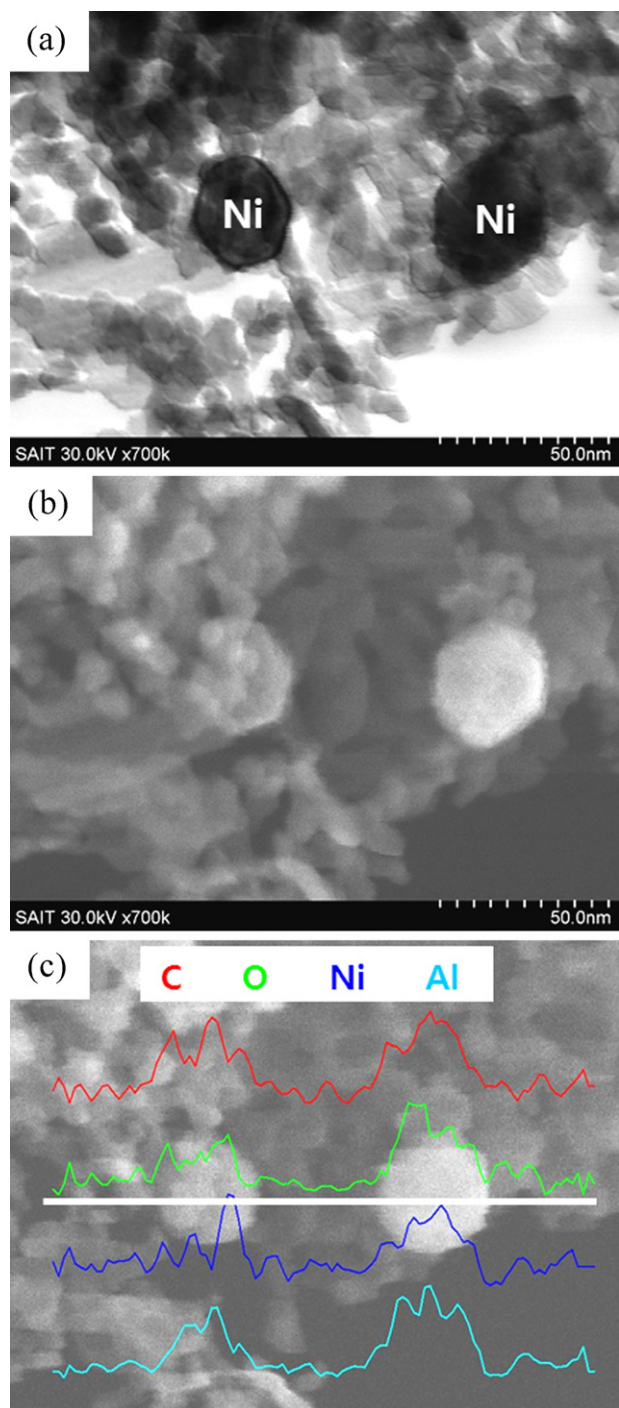
Fig. 9. (a) TEM, (b) SEM and (c) line-scan EDX analysis for used WNiAl catalyst at the same position. The used catalysts indicate after 200 h of combined reforming reaction of methane.

reported in previous studies [16,21]. Steam pretreatment reduced carbon deposition significantly at this early stage, and enhanced CH_4 and CO_2 conversion and long-term stability.

To elucidate the reason for the initial resistance to carbon deposition of steam pretreated catalysts, ^{27}Al NMR was performed; the results are shown in Fig. 5. The peak area ratio of tetrahedral Al (Al_{Td}) to octahedral Al (Al_{Oh}) is summarized in Table 1. The ratio decreased from 0.37 to 0.27 after the reforming reaction for the NiAl catalyst, while the ratio decreased from 0.38 to 0.33 for the WNiAl catalyst. Compared to the steam pretreated catalyst, the conventional NiAl catalyst showed a much larger reduction in the ratio

of Al_{Td}/Al_{Oh}, implying that more aluminum had leached from the framework. Leached aluminum often acts as a strong Lewis acid site that can cause severe carbon deposition [22]. The steam pretreatment might remove unstable aluminum from the catalyst in advance – aluminum that would be leached during the combined steam and carbon dioxide reforming of methane, leading to severe carbon deposition. Fig. 6 shows the NH_3-TPD results for the fresh catalysts before and after steam treatment. The catalysts were pretreated under He flow at 400 °C for 1 h. The total acidity greatly decreased after steam treatment from 511 μmol/g to 359 μmol/g. The steam treatment surely reduced the amount of acidic sites.

Fig. 7 demonstrates the TPR results before and after steam treatment. Whereas the Ni particle in fresh NiAl catalyst was reduced in low temperature of 100–400 °C, the Ni particle in fresh WNiAl catalyst after steam treatment was reduced at much higher temperature of 700–1000 °C. The metal-support interaction became much stronger, and SMSI (strong metal-support interaction) appeared after steam treatment. Fig. 8 shows the XPS (X-ray photoelectron spectroscopy) results for the catalysts. The Ni $2p_{2/3}$ and Al 2p peaks were shifted to higher binding energy after steam pretreatment. The interaction of Ni and alumina increased after steam pretreatment. The increased TOF after the reaction shown in Table 2 may result from the SMSI. Also, the stabilized WNiAl catalyst leached less Al and consequently exhibited less carbon deposition.

Additionally, we could obtain direct evidence showing that the Ni catalysts retained physical contact with their alumina support after steam pretreatment, although the particle size greatly increased. Fig. 9 demonstrates the results of ultra-high-resolution SEM/TEM dual mode microscopy showing images in both the scanning and transmission modes and energy-dispersive X-ray analysis in the same position. Ni particles are clearly visible in the TEM image in Fig. 9(a). When the same area was observed in a high-resolution scanning mode, as shown in Fig. 9(b), the surface of the Ni particles appeared to be partially covered by alumina. This observation was confirmed by line scan EDX analysis, as illustrated in Fig. 9(c). When the chemical composition (C, O, Ni, Al) was measured along the white line, alumina was located at the exactly same position as the Ni particles, which strongly indicates that these Ni particles are not isolated, but alumina supports surround the Ni particles. Although the size of Ni particles became larger after the steam treatment, the physical contact of Ni and alumina was retained, and their interaction actually became stronger as proved by TPR and XPS.

4. Conclusions

A simple pretreatment method was developed to enhance the carbon resistance of a Ni/γ-Al_2O_3 catalyst for the combined steam and carbon dioxide reforming of methane. When the Ni/γ-Al_2O_3 catalyst was treated with steam at high temperature before the reforming reaction, unstable aluminum that can leach and cause severe carbon deposition at early stages of the reaction was stabilized in advance. The metal-support interaction became stronger after steam treatment as confirmed by TPR and XPS. The resulting Ni/γ-Al_2O_3 catalyst showed the thermodynamically possible highest conversion of methane (98.3% at 850 °C) and was operated stably for 200 h at the same temperature without notable deposition of wire-type carbon coke. This simple pretreatment could be applied for commercial Ni/Al_2O_3-based catalysts with enhanced activity and long-term stability, and possibly can be applied for other alumina-based catalysts.

References

[1] C.S. Song, Catalysis Today 115 (2006) 2–32.
[2] Y.X. Pan, P.Y. Kuai, Y.A. Liu, Q.F. Ge, C.J. Liu, Energy and Environmental Science 3 (2010) 1322–1325.
[3] N.N. Sun, X. Wen, F. Wang, W. Wei, Y.H. Sun, Energy and Environmental Science 3 (2010) 366–369.
[4] M.S. Fan, A.Z. Abdullah, S. Bhatia, Applied Catalysis B: Environmental 100 (2010) 365–377.
[5] F. Yagi, R. Kanai, S. Wakamatsu, R. Kajiyama, Y. Suehiro, M. Shimura, Catalysis Today 104 (2005) 2–6.
[6] H.S. Roh, K.Y. Koo, U.D. Joshi, W.L. Yoon, Catalysis Letters 125 (2008) 283–288.
[7] D.L. Hoang, S.H. Chan, O.L. Ding, Chemical Engineering Journal 112 (2005) 1–11.
[8] K.Y. Koo, H.S. Roh, Y.T. Seo, D.J. Seo, W.L. Yoon, S. Bin Park, International Journal of Hydrogen Energy 33 (2008) 2036–2043.
[9] H.W. Chen, C.Y. Wang, C.H. Yu, L.T. Tseng, P.H. Liao, Catalysis Today 97 (2004) 173–180.
[10] Z.Y. Hou, O. Yokota, T. Tanaka, T. Yashima, Applied Surface Science 233 (2004) 58–68.
[11] S.H. Seok, S.H. Choi, E.D. Park, S.H. Han, J.S. Lee, Journal of Catalysis 209 (2002) 6–15.
[12] J.G. Zhang, H. Wang, A.K. Dalai, Journal of Catalysis 249 (2007) 300–310.
[13] D.P. Liu, X.Y. Quek, W.N.E. Cheo, R. Lau, A. Borgna, Y.H. Yang, Journal of Catalysis 266 (2009) 380–390.
[14] M.A. Goula, A.A. Lemonidou, A.M. Efstathiou, Journal of Catalysis 161 (1996) 626–640.
[15] M.C.J. Bradford, M.A. Vannice, Applied Catalysis A: General 142 (1996) 73–96.
[16] V.C.H. Kroll, H.M. Swaan, C. Mirodatos, Journal of Catalysis 161 (1996) 409–422.
[17] H.S. Li, J.F. Wang, Chemical Engineering Science 59 (2004) 4861–4867.
[18] S.B. Wang, G.Q. Lu, Applied Catalysis B: Environmental 19 (1998) 267–277.
[19] J.H. Kim, D.J. Suh, T.J. Park, K.L. Kim, Applied Catalysis A: General 197 (2000) 191–200.
[20] B. Fidalgo, A. Arenillas, J.A. Menendez, Applied Catalysis A: General 390 (2010) 78–83.
[21] A.M. Amin, E. Croiset, W. Epling, International Journal of Hydrogen Energy 36 (2011) 2904–2935.
[22] A. de Lucas, P. Canizares, A. Duran, A. Carrero, Applied Catalysis A: General 154 (1997) 221–240.